Interaction grand potential between calcium-silicate-hydrate nanoparticles at the molecular level (Supporting Information)

Patrick A. Bonnaud,*[a] Christophe Labbez,[b‡] Ryuji Miura,[a] Ai Suzuki,[a] Naoto Miyamoto,[a] Nozomu Hatakeyama,[a] Akira Miyamoto,[a] and Krystyn J. Van Vliet[c]

S1. Validation of force computation for a system of two interacting ions.

To validate our algorithm computing forces between C-S-H particles, we used a simple system made of two ions in a cubic simulation box of a width 3.11 nm. Dispersion-repulsion forces between ions are modelled with a Lennard-Jones potential and we took parameters corresponding to a CH_4 molecule ($\sigma = 0.371$ nm and $\varepsilon = 1.2644$ kJ.mol)[1]. For partial charges, one ion carry a positive charge ($+1e$), while the other one carry a negative charge ($-1e$). We called EW1, EW2, and EW3 the real part, the reciprocal part, and the dipole contribution to Ewald forces. We compared our computation results with data obtained on the same system with the DL_POLY Molecular Simulation Package (version 2.19)[2]. Results are shown in Fig. 1. We observed a good agreement between our computations and data computed with DL_POLY. A small discrepancy is observed for $D > 0.6$ nm. The difference is due to the use of the dipole correction (EW3), which is not included in Ewald forces computed with DL_POLY.

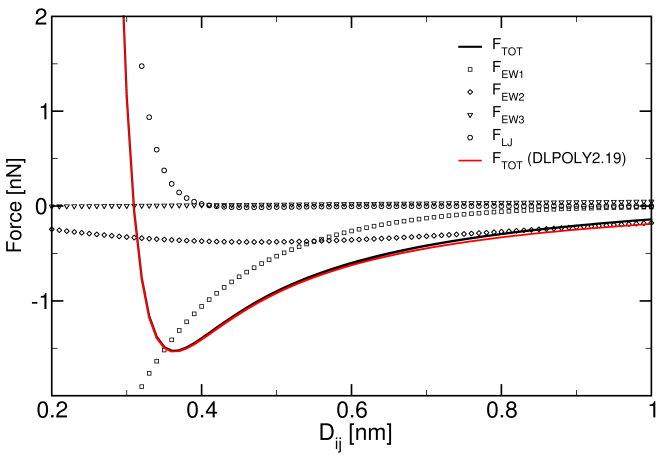

Fig. 1 Forces between two opposite charged ions as a function of the distance D_{ij}. The red solid line is the total force between ions computed with the DL_POLY Molecular Simulation Package (version 2.19)[2]. The black solid line is the total force between ions computed with our homemade code. Empty squares, empty diamonds, empty down triangles, and empty circles stand for the real space contribution to ewald forces (EW1), the reciprocal space contribution to Ewald forces (EW2), the dipole contribution to Ewald forces (EW3), and the Lennard-Jones forces, respectively.

S2. Excess potential energy

Figure 2 shows the excess potential energy $\Delta U = U(D) - U(D_{\max})$ as a function of the distance between C-S-H particle pairs for configurations A, B, and C ($D_{\max} = 6.36$ nm). The reference potential energy $U(D_{\max})$ was -506.76×10^5 kJ/mol (configuration A), -504.88×10^5 kJ/mol (configuration B), and -506.77×10^5 kJ/mol (configuration C). For each interparticle configuration considered, the minimum in excess potential energy corresponded to the maximum N_{water} in Fig. 3 of the main article. For configurations A and B, this potential energy minimum occurred at the same distance D_{ij} between C-S-H particles ($D_{ij} \sim 3.16$ nm). The absolute number of water molecules in both configurations was similar ($N_{\text{water}} \sim 3550$ molecules), but the absolute potential energy minimum was lower by 1.91×10^5 kJ/mol in configuration A. Configuration B was established to probe the effect of in-plane misorientation of the silicate-rich surfaces of the particle pairs. Here, we observed that this in-plane rotation between the particles negligibly affected the water content, but did increase the total potential energy. Finally, for configuration A the inter-lamellar equilibrium distance (∼0.49 nm) at 10% RH was found by subtracting from the distance at the excess potential energy minimum (∼3.16 nm) the distance at zero excess potential energy, ∼2.67 nm (see Fig. 2). This is similar to the spacing found at higher humidity levels (∼0.5 nm). This is expected in that the water content between two facing C-S-H particles and within C-S-H particles changes only slightly at humidity greater than 10% RH[3].

Furthermore, for configuration C, the potential energy minimum occurred at larger separation distances, $D_{ij} \sim 4.87$ nm. This difference is attributable to the c_{part}:a_{part} particle aspect ratio that reduced the gap between particle pair surfaces d_{ij} for the same distance D_{ij} in configuration C. Indeed, insets in Fig. 2a show results as a function of d_{ij}, the distance between opposing free surfaces, to distinguish these effects. We observed that minima in potential energies were similar among all particle pair configurations, and appeared in the range $0.65 < d_{ij} < 0.9$ nm, with the lowest distance being for configuration C. Note that negative values for d_{ij} were possible due to our definition of the location of free surfaces, which we defined by the furthest oxygen atom in silica chains with respect to the center of mass of the particle in each direction (a, b, and c). The absolute number of water molecules in configuration C was similar to configurations A and B (∼3550), while the absolute potential energy minimum was roughly ∼3906 kJ/mol higher than that in configuration A, but $\sim 1.87 \times 10^5$ kJ/mol lower than

[a] *Miyamoto Laboratory, New Industry Creation Hatchery Center, Tohoku University, Sendai, Miyagi, Japan. Fax: +81 22 795 7235; Tel: +81 22 795 7233; E-mail: patrick@aki.niche.tohoku.ac.jp*
[b] *Laboratoire Interdisciplinaire Carnot de Bourgogne, UMR 6303, CNRS - Univ. Bourgogne Franche-Comté, F-21078, Dijon, France.*
[c] *Department of Materials Science and Engineering, Massachusetts Institute of Technology, Cambridge, MA 02139, USA.*

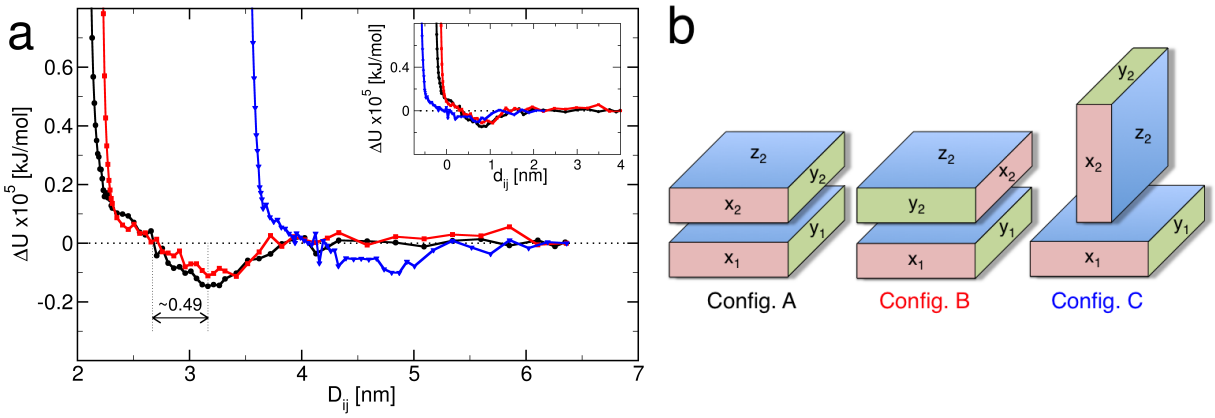

Fig. 2 (a) Excess potential energy $\Delta U = U(D_{ij}) - U(D_{\max})$ as a function of the distance D_{ij} between interacting calcium-silicate-hydrate particles ($D_{\max} = 6.36$ nm). Black filled circles, red filled squares, and blue filled down triangles correspond to configurations A, B, and C, respectively. Insets in a shows results as a function of d_{ij}, the distance between opposing free surfaces. For configuration A, we extracted the inter-lamellar equilibrium distance ($\sim$0.49 nm) by subtracting from the distance at the excess potential energy minimum $\sim$3.16 nm the distance at zero excess potential energy $\sim$2.67 nm. (b) Cartoons showing the calcium-silicate-hydrate (C-S-H) particle pairs in configurations A, B, and C. $\{x_1, y_1, z_1\}$ and $\{x_2, y_2, z_2\}$ refer to surface normals for particle 1 (bottom) and particle 2 (top), respectively.

in configuration B. Therefore, potential energy results suggest that configuration A has the highest probability to be found in nature among the configurations we explored, and that configuration C is more energetically favored than configuration B. Nevertheless, in the latter classification of configurations based on potential energy, we neglected the effect of the entropy that usually plays an important role for non-null temperatures and the grand canonical term $\mu_{\text{water}} N_{\text{water}}$. Interaction grand potentials are better suited for such comparison.

Finally, we observed a change of slope in the repulsive portion of the potential energy profile at $D_{ij} \sim 2.3$ nm for configurations A and B, and at $D_{ij} \sim 3.7$ nm for configuration C. This slope change is attributable to onset of repulsion among atoms within the silica chains of each particle that contribute at sufficiently small D_{ij}; as noted in Methods, the positions of atoms within silica chains were maintained fixed upon mutual approach of C-S-H particles, whereas atoms comprising water molecules and the calcium and oxygen atoms that were not bonded to silica chains were free to displace.

S3. Cumulative charge densities

Cumulative charge densities are shown in Fig. 3.

S4. Different contributions in interaction grand potentials

Figure 4 show the different contributions in interaction grand potentials, i.e., water-particle interactions, calcium counterion-particle interactions, particle-particle interactions, and the grand canonical term. In the water-particle contribution to interaction grand potentials, oscillations are found in the range $2 \leq D_{ij} \leq 4.5$ nm and their periods are increasing with D_{ij} (except for the last oscillation). Oscillation periods are on the same order of magnitude for configurations A and B. Nevertheless, for configuration B oscillations are shifted to higher D_{ij} values. When summing calcium counterion-particle and particle-particle contributions to

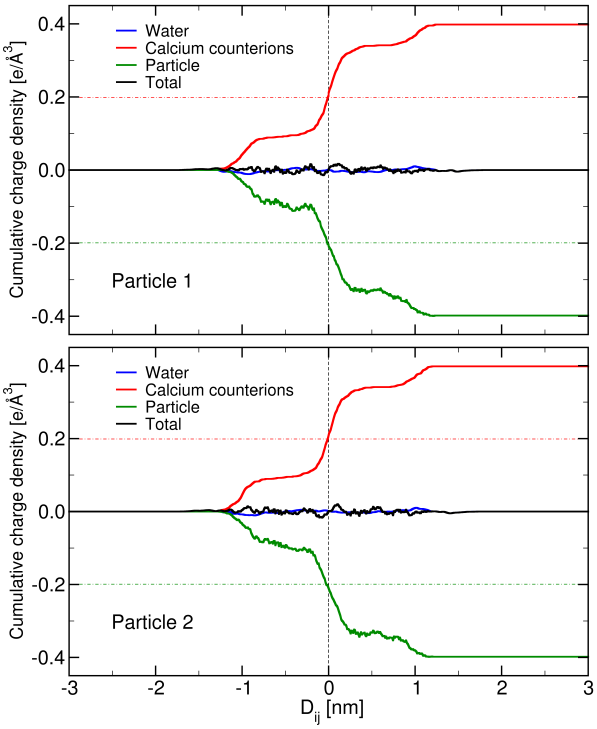

Fig. 3 Cumulative charge densities for particle 1 (top; the reference particle) and particle 2 (bottom; the moving particle). Thick black solid lines, thick blue solid lines, thick red solid lines, thick green solid lines stand for the total cumulative charge density, the water contribution, the calcium counterion (C_w) contribution, and the particle contribution to the cumulative charge density. Calcium ions (Ca), oxygen atoms (O), and silicon atoms (Si) are included in the particle contribution. The vertical black dotted line is the particle center of mass. Red and green horizontal dashed dotted lines show half of the total charge density for calcium counterions and the particle, respectively.

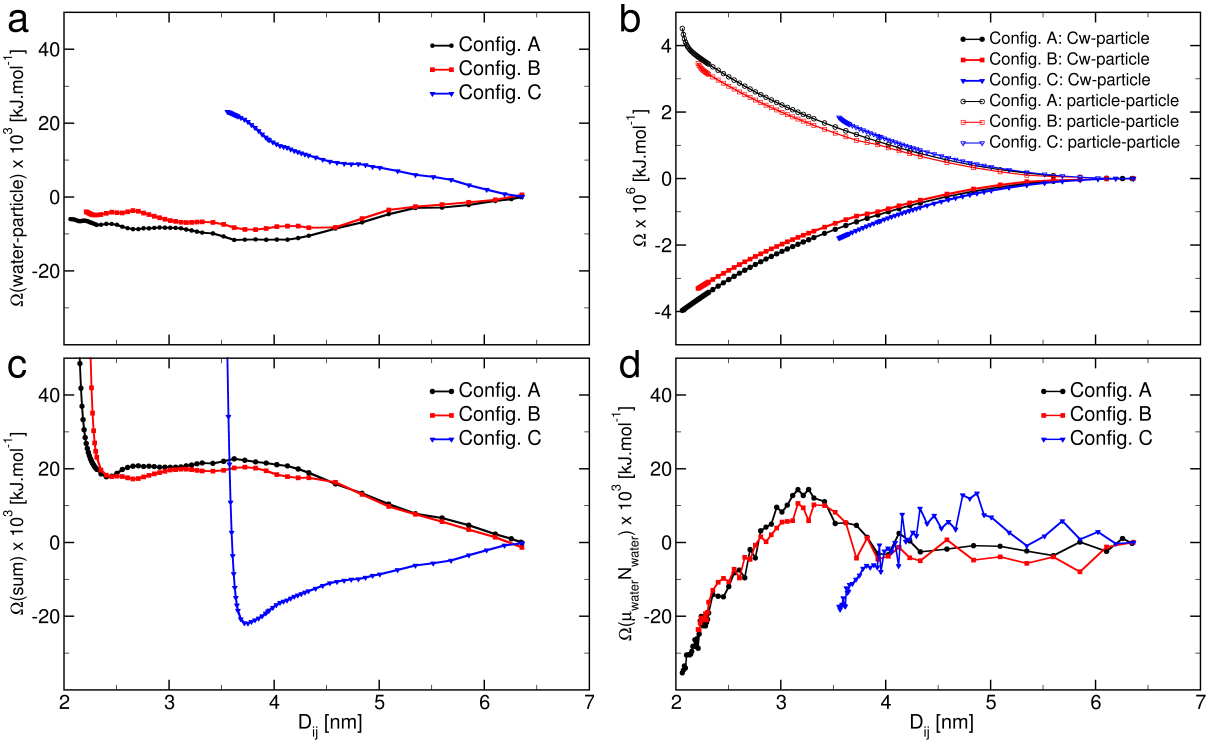

Fig. 4 (a) Contribution of water-particle interactions to interaction grand potentials; (b) contributions of calcium counterion-particle interactions (filled symbols) and particle-particle interactions (empty symbols) to interaction grand potentials; (c) sum of calcium counterion-particle and particle-particle contributions to interaction grand potentials; and (d) contribution of the grand canonical term to interaction grand potentials. Black circles, red squares, and blue down triangles stand for configurations A, B, and C, respectively.

interaction grand potentials, we also observed oscilations in the range $2 \leq D_{ij} \leq 4.5$ nm. Amplitude of oscillations are overall small and annihilated in total interaction grand potentials by the grand canonical term and its large statistical fluctuations. We do not observe oscillations in water-particle interactions for configuration C due to the small interacting surface area (~ 9.95 nm^2) and the different nature of surfaces. For configurations A and B, water-particle and calcium counterion-particle contributions exhibit negative values on the whole reaction path contributing to the overall cohesive behavior. For configuration C, water-particle interactions exhibit positive values reducing the overall cohesion, while calcium counterion-particle contributions exhibit negative values as for configurations A and B. For the three configurations, particle-particle contributions exhibit positive values reducing the overall cohesive behavior. Finally, the grand canonical term exhibit a maximum corresponding to the location of the maximum of water molecules for each configuration and contributes to the cohesion among particles for distances below $\sim$3 nm for configurations A and B and below $\sim$4 nm for configuration C.

S5. Different contributions in mean forces

Different contributions in mean forces are shown in Fig. 5 and Tab. 1.

S6. Relative contribution of surface orientation

The construction of interaction grand potentials can be used to describe interactions between discrete particles, which naturally includes contributions from both the particle geometry (e.g., aspect ratios that affect the relative size of opposing surface areas) and the relative surface area orientation. If one seeks instead to compare the relative stability and cohesion between specific surface misorientations (e.g., for design of idealized experiments or for representation of C-S-H as continuous yet disordered layers), then the above interaction grand potentials can be expressed per unit of the interacting surface area (S_{int}) as a function of d_{ij}. Figure 6 provides this representations. For configurations A and B, the interacting surface area is $S^A_{\text{int}} = S^B_{\text{int}} \sim 26.15$ nm^2, while it is $S^C_{\text{int}} \sim 9.95$ nm^2 for configuration C. We obtained values of the interaction grand potential well-depths (~ -337.04 kJ.mol^{-1}.nm^{-2}, $\sim$34.9 kJ.mol^{-1}.nm^{-2}, and ~ -1093.47 kJ.mol^{-1}.nm^{-2} for configurations A, B, and C, respectively). Configurations C show the deepest well-depth indicating that this configuration among C-S-H surfaces have the strongest cohesive behavior among those considered, while configuration B has a well-depth in positive energies and thus is least cohesive. Comparison of configurations A and B show that surface misorientation affects cohesion between surfaces. As in the consideration of discrete particle geometry, the surfaces were more cohesive when aligned parallel (configuration A), since that it is essentially a continuation of the C-S-H unit (stacking of C-S-H layers); configuration B includes a stacking fault making

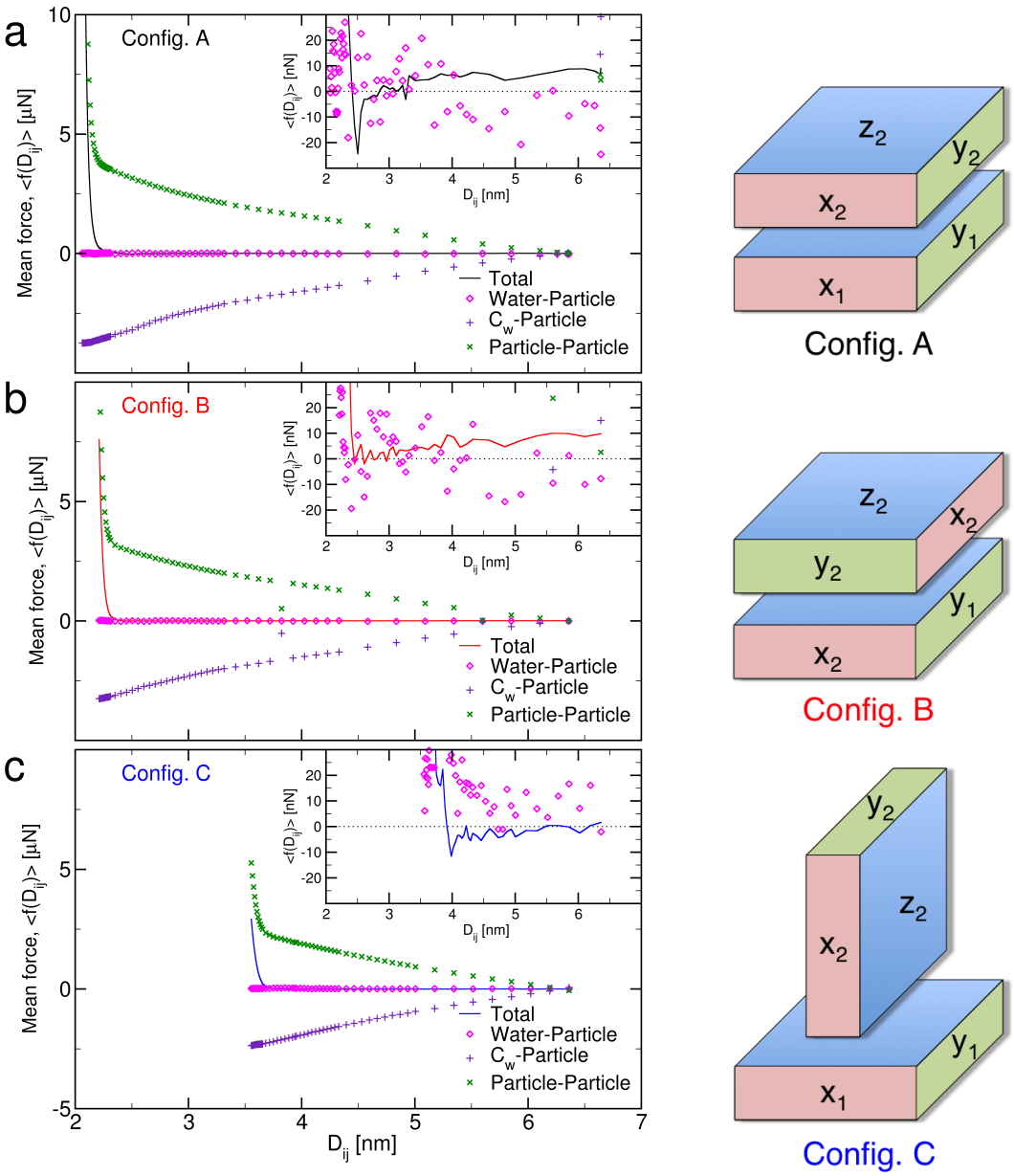

Fig. 5 Mean computed forces between calcium-silicate-hydrate particles as a function of D_{ij}, the distance between centers of mass, along the reaction path. Three configurations are investigated: (a) configuration A with black solid lines, (b) configuration B with red solid lines, and (c) configuration C with blue solid lines. Molecular details of these configurations can be found in Fig. 1 of the main article and cartoons are shown on the right side of the figure. $\{x_1, y_1, z_1\}$ and $\{x_2, y_2, z_2\}$ refer to surface normals for particle 1 (bottom) and particle 2 (top), respectively. By 'Particle', we refer to atoms belonging to particles, which includes Si, O, and Ca atoms. Magenta empty diamonds, indigo plusses, and green crosses stand for the water-particle contribution to the mean forces, the calcium counterions (C_w)-particle contribution to the mean forces, and the particle-particle contribution to the mean forces, respectively. Insets show results at a smaller scale on the y-axis in order to see variations of the total mean forces.

Table 1 z-components of mean forces at the maximum interparticle distance, $D_{\max}$.

Configuration	z-component of mean forces [nN]		
	Water-Particle	Calcium counterions-Particle	Particle-Particle
A	−24.69	29.19	4.47
B	−5.98	13.77	1.95
C	−0.62	61.84	−59.55

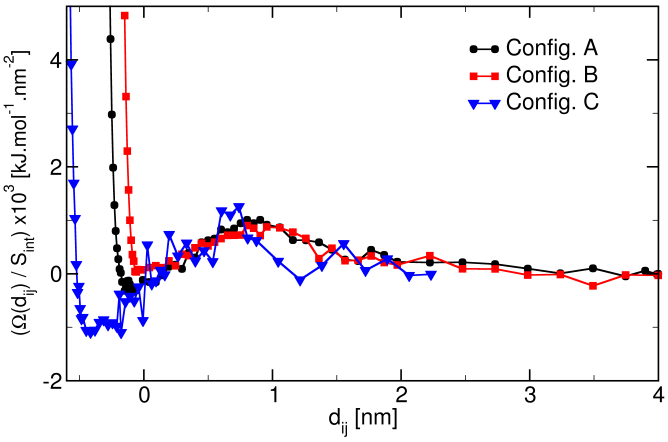

Fig. 6 Interaction grand potentials computed by mean force integration for calcium-silicate-hydrate particles, per unit of the mean interacting surface area as a function of d_{ij}, the distance between interacting surfaces. Simulation data are shown for configurations A (black filled circles), B (red filled squares), and C (blue filled triangles).

the system much less cohesive. Furthermore, comparison of configurations A and C show that the latter surface orientation exhibit stronger cohesive properties, and that considering the particle geometry in the interaction grand potentials reduces the relative cohesion among geometrically irregular particles. This comparison of C-S-H surface misorienations and particle geometry on particle interaction energies emphasizes the importance of taking into account C-S-H particle dimensions in descriptions of physical and simulated multiparticle or mesoscale systems.

References

1 D. Trzesniak, A.-P. E. Kunz and W. F. van Gunsteren, *ChemPhysChem*, 2007, **8**, 162–169.

2 W. Smith and T. R. Forester, *Journal of Molecular Graphics*, 1996, **14 (3)**, 136–141.

3 P. Bonnaud, Q. Ji, B. Coasne, R. J.-M. Pellenq and K. J. V. Vliet, *Langmuir*, 2012, **28**, 11422.